Vortex flipping in superconductor/ferromagnet spin-valve structures

E. J. Patiño,[1] M. Aprili,[2] M. G. Blamire,[3] and Y. Maeno[4]

[1]*Departamento de Física, Grupo de Física de la Materia Condensada, Universidad de los Andes, Bogotá, Colombia*

[2]*Laboratoire de Physique des Solides, UMR8502, Bâtiment 510, Université Paris-Sud, 91405 ORSAY Cedex, France*

[3]*Department of Material Science and Metallurgy, University of Cambridge, Pembroke Street, Cambridge CB2 3QZ, United Kingdom*

[4]*Department of Physics, Graduate School of Science, Kyoto University, Kyoto 606-8502, Japan*

(Received 8 March 2012; revised manuscript received 16 May 2013; published 20 June 2013)

We report in-plane magnetization measurements on Ni/Nb/Ni/CoO and Co/Nb/Co/CoO spin valve structures with one of the ferromagnetic layers pinned by an antiferromagnetic layer. In samples with Ni below the superconducting transition T_c, our results show strong evidence of vortex flipping driven by ferromagnet magnetization. This is a direct consequence of the proximity effect that leads to vortex supercurrent leakage into the ferromagnets. Here, the polarized electron spins are subject to the vortices' magnetic field, occasioning vortex flipping. Such a novel mechanism has been made possible by fabrication of the ferromagnet/superconductor/ferromagnet/antiferromagnet multilayered spin valves with an S layer thin enough to barely confine vortices inside as well as F layers thin enough to align and control magnetization within the plane. When Co is used, the vortex flipping effect is not observed. This is attributed to the shorter coherence length of Co. Interestingly, a reduction in the pinning field of about 400 Oe is observed instead when the Nb layer is in the superconducting state. This effect cannot be explained in terms of vortex fields. In view of these facts, any explanation must be directly related to the proximity effect and thus a remarkable phenomenon that deserves further investigation.

DOI: 10.1103/PhysRevB.87.214514 PACS number(s): 74.25.Ha, 74.45.+c, 75.30.Et

I. INTRODUCTION

Superconductor (S) ferromagnet (F) multilayered structures have been a subject of intensive research in the past decade because of the new physical properties that arise in the superconductor by placing it next to a ferromagnet. So far, it has been established experimentally that there can be three ways to modify the superconducting properties in S/F structures: first by the usual proximity effect (i.e., Cooper pair penetration into the ferromagnet), second by the inverse proximity effect),[1–3] and third by stray fields coming from the ferromagnet Bloch domain walls or magnetic poles from the sample edges.[4]

For the case of the proximity effect, when Cooper pairs penetrate into the ferromagnet, they experience the ferromagnet's exchange field generating the so-called Fulde–Ferrel–Larkin–Ovchinnilov (FFLO) state.[5,6] In this state, the real part of the order parameter penetrates the ferromagnet a distance on the order of the coherence length ξ_F and oscillates due to dephasing by the exchange energy of the ferromagnet. This leads to the oscillations of the superconducting transition temperature (T_c) as a function of ferromagnet thickness[7–11] and π phase shift in S/F junctions.[12,13] Furthermore, recent measurements in S/F structures[11,14–16] have provided evidence for triplet pairing in the ferromagnet induced by noncollinear magnetizations of the F layers.

Regarding effects due to stray fields, these may come from either domain walls or magnetic poles, which pierce the superconductor. When an S/F heterostructure is subjected to an externally applied field, the ferromagnet magnetization transits from a multidomain to a single-domain state. When the ferromagnet is in the single-domain state, effects from dipole stray fields may be significant. Evidence of these has been reported for Co/Nb/Co trilayer structures with thick Co layers measured by magnetization and critical current measurements.[17,18] In a multidomain state, the overall domain configuration is what gives the net magnetization; in particular at coercive fields, this configuration is such that the overall magnetization is zero.

Domain walls can be classified into two types, Neel and Bloch, in which the magnetization lies in the surface plane and out-of-plane direction, respectively. For thick ferromagnets, Bloch domain walls may generate vortices in the superconductor in the out-of-plane direction, affecting its critical current (see Ref. 19, and references therein). As the ferromagnet thickness decreases, demagnetizing fields increase, which means that it becomes increasingly energetically favorable for domain walls to mutate from the out-of-plane to in-plane direction. This has been demonstrated in experiments in Co, Permalloy (Py), and Ni samples,[19–22] where it has been observed that the transition between these two types of domain walls occurs at around 30 nm for Co and 20 nm for Ni.

In experiments where effects due to FFLO state were investigated,[5–13] the chosen ferromagnet thickness was on the order of the ferromagnet coherence length. In most ferromagnetic metals and alloys, this corresponds to a few nanometers. In this range one usually expects domain walls to lie in the plane.

On the contrary, experiments where the thickness of the ferromagnet was much greater than the ferromagnet coherence length, effects due to Bloch domain walls were observed (see Ref. 19, and references therein). In this case, FFLO effects, damped at the ferromagnet coherence length scale, are too small to be measurable at this thickness range.

Concerning the superconductor dimensions, it is well known that for thin films, T_c falls below its bulk value as the superconductor gets thinner. Therefore in most S/F experiments, the main criterion for choosing its thickness usually was a high enough T_c value to be measurable by the available apparatus.

In this paper, we present magnetization measurements on F/S/F/antiferromagnet (AF) spin valve structures where either

Co or Ni is used as the F layer, CoO as the AF layer, and Nb as the superconductor. The ferromagnet thickness was chosen larger than the ferromagnet coherence length to avoid FFLO state effects, but thin enough to prevent Bloch domain wall effects. The superconductor thickness was chosen smaller than the vortex core diameter and thus constitutes one of the main parameters of our investigation.

We show that under these conditions, Ni magnetization is able to flip vortices. On the other hand, when Co is used, vortex flipping effects are absent and instead a reduction in pinning field is observed.

Prior to performing magnetization measurements on spin valve structures, a reference Nb/Co bilayer structure was studied. This sample was grown by sputtering technique, producing a Nb film with a thickness larger than the vortex core radius. This makes this Nb/Co bilayer a good reference sample for our subsequent magnetization measurements.

II. EXPERIMENT

A. Nb/Co bilayers

The Nb/Co bilayers were grown using an ultrahigh vacuum (UHV) DC-magnetron sputtering system in a chamber cooled to $-100\,^{\circ}$C using liquid nitrogen. The base pressure was less than 2×10^{-9} Torr. The partial oxygen base pressure in the chamber measured using a mass spectrometer was less than 0.7×10^{-11} Torr. The Nb and Co sputtering targets were 99.95% pure, deposited under Ar pressure of 3.7×10^{-3} Torr in an in-plane magnetic field of approximately 400 Oe. The bilayer sample was grown on Si (100) substrates, with a Nb thickness $d_{\mathrm{Nb}} = 25$ nm.

Given the ferromagnet's thickness, we expect the usual proximity effect due to Cooper pair penetration without stray field effects from domain walls. The superconducting transition temperature T_c of the Nb/Co sample was determined by four-point resistivity measurements to be 6.4 K. T_c was defined as the value where the resistance drops to half of the resistance above transition. The transition width found this way was of 0.1 K for this sample. From resistivity measurements, the mean free path of a Nb film with a thickness of 25 nm was determined to be about 3 nm. Using the expressions; $\xi_S = (\hbar D_S/2\pi k_b T_c)^{1/2}$ and $\xi_{GL}(0) = \pi\xi_S/2$; the superconducting coherence length $\xi_S \sim 7$ nm and Ginzburg Landau coherence $\xi_{GL} \sim 11$ nm were obtained, respectively. Here, D_S is the diffusion coefficient calculated using a Fermi velocity $v_F = 2.77 \times 105$ m/s (Ref. 23).

This corresponds to the vortex core radius giving an estimate of the vortex core diameter $2\xi_{GL} \sim 22$ nm smaller than the Nb layer thickness.

The traveled length of Cooper pairs into the ferromagnet or the ferromagnetic coherence length of $\xi_{Co} \sim 0.3$ nm was found using the expression $\xi_F = \hbar v_F/2I$, where I represents the ferromagnet exchange energy.

Magnetization measurements on this sample were performed with the field parallel to the film surface using a superconducting quantum interference device magnetometer (Quantum Design MPMS). The measurements were carried out in "DC and no overshoot" mode on samples with dimensions of 5×5 mm^2. Before starting the measurements, the magnet was cycled down from 6000 Oe to 0 using an oscillating field sequence in order to remove any trapped flux in the superconducting magnet.

B. Ni/Nb/Ni/CoO and Co/Nb/Co/CoO spin valve structures

These spin valve structures were grown using a UHV e-gun evaporation system entirely *in situ*. The base pressure was better than 1×10^{-9} Torr, and the evaporation pressure was less than 2×10^{-8} Torr. The film thickness was monitored during growth to better than 1 Å by quartz balance. The multilayered structures were grown on Si (100) substrate. Using this growth technique, the Nb mean free path is about 9 nm, as obtained from previous resistivity measurements.[24] This results in a larger superconducting coherence length $\xi_S \sim 12$ nm. From this value we can estimate the order of the Ginzburg Landau coherence length $\xi_{GL} \sim 19$ nm. This corresponds to a vortex core diameter $2\xi_{GL} \sim 38$ nm larger than the superconductor thickness.

In our Ni(3)/Nb(25)/Ni(3)/CoO(2)/Nb(4) sample, where the numbers in parenthesis indicate thickness in nanometers, the first layer thickness was Ni of 3 nm then Nb of 25 nm deposited at a high deposition rate of about 7 Å/s. Then a 3-nm Ni layer followed by 2 nm of Co were grown prior to oxidizing the Co for 120 seconds in a 1×10^{-2} Torr oxygen pressure.

Finally, a 4-nm Nb layer was deposited as a capping layer. The Ni thickness $d_{Ni} = 3$ nm is approximately twice the ferromagnetic coherence length $\xi_{Ni} \sim 1.2$ nm in the dirty limit,[25] so we expect Cooper pairs to penetrate to almost half the entire Ni thickness. Also, the small thickness of the ferromagnet implies that domain walls lie in-plane,[20] eliminating stray field effects from domain wall formation.

Our Co(2.5)/Cu(5)/Nb(25)/Cu(5)/Co(2.5)/CoO(2.5)/Al(10) sample was grown under very similar deposition rates and oxidation parameters as our sample with Ni. The Cu layers were included in order to eliminate intermixing of Co and Nb atoms and thus improve the interface quality.[26] Its narrow thickness, compared with Cooper pair penetration in a normal metal (∼64 nm),[27] does not significantly change the proximity effect into the ferromagnet.

Magnetization measurements on these samples, with dimensions of 10×5mm^2, were performed by the same method employed for the Nb/Co bilayer. Before starting the measurements, the magnet was quenched in order to remove any trapped flux in the superconducting magnet.

III. MAGNETIZATION MEASUREMENTS

A. Nb/Co bilayers

Magnetization measurements on Nb/Co bilayer structures made at room temperature showed coercive fields of about 20 Oe (see lower inset to Fig. 1). Then the sample was cooled down, and the characteristic magnetization loop of a type II superconductor was obtained at 5 K (see Fig. 1). Here, a value of $H_{c1\parallel} = 100$ Oe at 4.2 K is obtained from the hysteresis loop where the magnetization slope loses its Meissner linear behavior.

In this curve, we clearly see the tree characteristic vortex processes of a type II superconductor: vortex penetration,

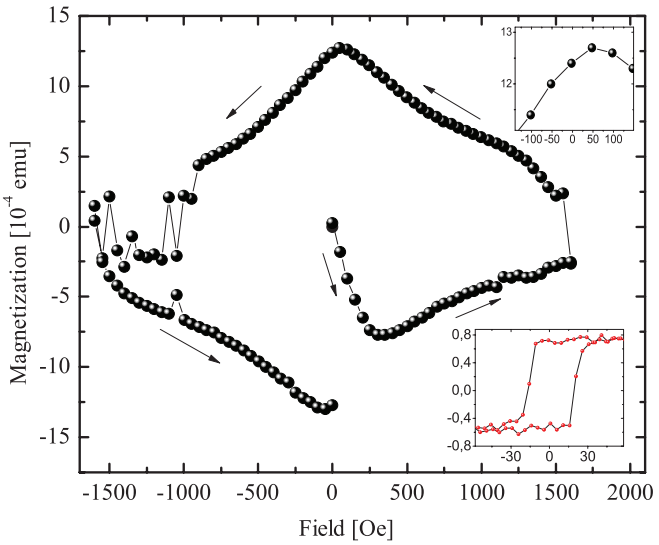

FIG. 1. (Color online) Hysteresis loop of a Nb(25 nm)/Co(3 nm). Upper inset shows peak position shift of 50 Oe relative to the zero position taken at 4.2 K. Lower inset shows hysteresis loop at room temperature.

vortex pinning, and vortex creation-annihilation. This last process may lead to flux jumps, as observed in Fig. 1, due to spontaneous vortex creation-annihilation and heat release processes[28] characteristic of in-plane measurement configuration. It is worth pointing out that the Nb/Co sample shows a shift of the central peak position near zero field toward a positive field of about 50 Oe (see upper inset in Fig. 1). According to Ref. 17, this indicates the presence of dipole stray fields from the magnetic layers that are still smaller than H_{c1}.

B. Ni/Nb/Ni/CoO spin valve structures

In order to reduce dipole stray fields, Ni/Nb/Ni/CoO multilayered structures were investigated using Ni as the ferromagnet given its lower saturation magnetization compared with Co.

Starting at a temperature of 350 K, above the AF Néel temperature $T_N = 291$ K of the CoO layer, the sample was cooled in a field of 500 Oe down to 5 K. This process permitted the ferromagnet to be exchange-biased in the applied field direction. At 5 K the external field was switched off, and the sample was cooled in zero field while the magnetization as a function of temperature was recorded. The superconducting transition temperature obtained in this way was around 2.5 K.[29]

Figure 2(a) shows in-plane magnetization curves above and below T_c (red and blue dots, respectively, in online version). These were taken starting at high fields. Above T_c, the magnetization curves show a Ni coercive field of about ±40 Oe and a small kink between ±50 and ±500 Oe on increasing field direction. This field range corresponds to the pinning of one of the Ni layers with the neighboring CoO film. Here the pinned Ni layer gradually rotates from an antiparallel toward a parallel configuration. This has similar characteristics to the one obtained in Ref. 30. Around the Ni coercive field, the magnetization of the ferromagnetic layers is in the antiparallel configuration, as shown in Fig. 3(a) (zoom view).

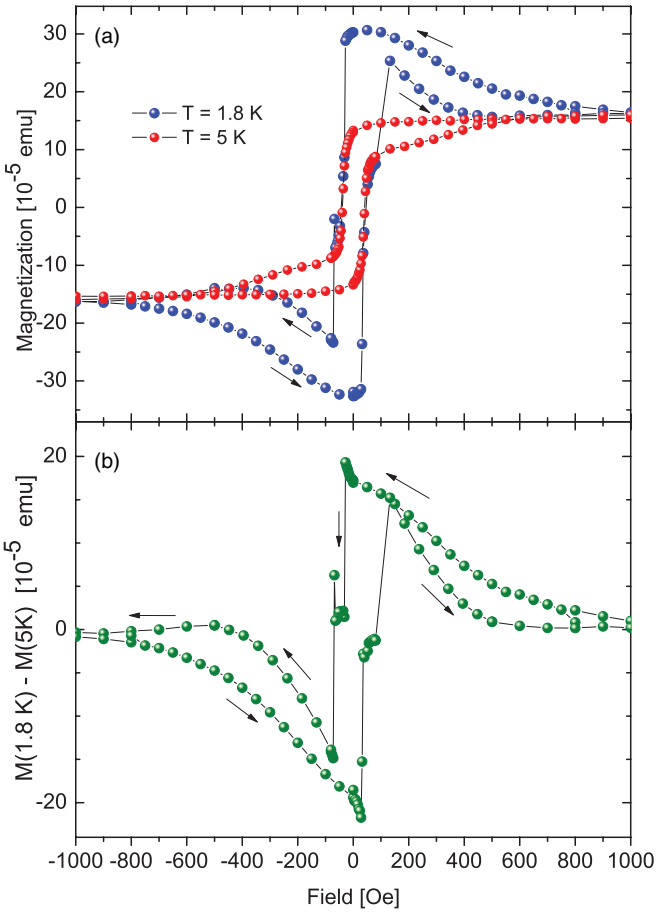

FIG. 2. (Color online) (a) Magnetic hysteresis loops of Ni(3)/Nb(25)/Ni(3)/CoO(2)/Nb(4) above and below T_c. (b) Hysteresis loop of the superconducting magnetization for the same sample measured along the plane after cooling in zero field. Here the magnetization at 5 K has been subtracted.

Below T_c the superconductor adds a magnetic contribution to the signal. In order to clearly extract the Nb superconducting signal from the total signal, the magnetization at T = 5 K is subtracted from the magnetization at T = 1.8 K. The Nb signal obtained this way is shown in Figs. 2(b) and 3(b) (zoom view). Here, the signal has maxima just below coercive fields of the ferromagnets. As anticipated, the superconductor signal of the spin valve in Figs. 2(b) and 3(b) is quite different from that in a simple F/S bilayer in Fig. 1. Starting at high positive fields, decreasing the field and changing its direction at zero field, the magnetization increase corresponds to vortex pinning in the positive field direction. This flux trapping continues up to the Ni coercive field.

Around this field, when the unpinned Ni layer switches, the sample magnetization drops to nearly zero [see inset of Figs. 2(b) and 3(b)]. This can only be explained as about half of the vortices flip following the free Ni layer.

By further increasing the field amplitude in the negative direction at about −65 Oe, the superconductor's magnetization abruptly switches sign, indicating flipping of the remaining vortices along the negative field direction [see inset of Figs. 2(b) and 3(b)]. This occurs in the field range where the

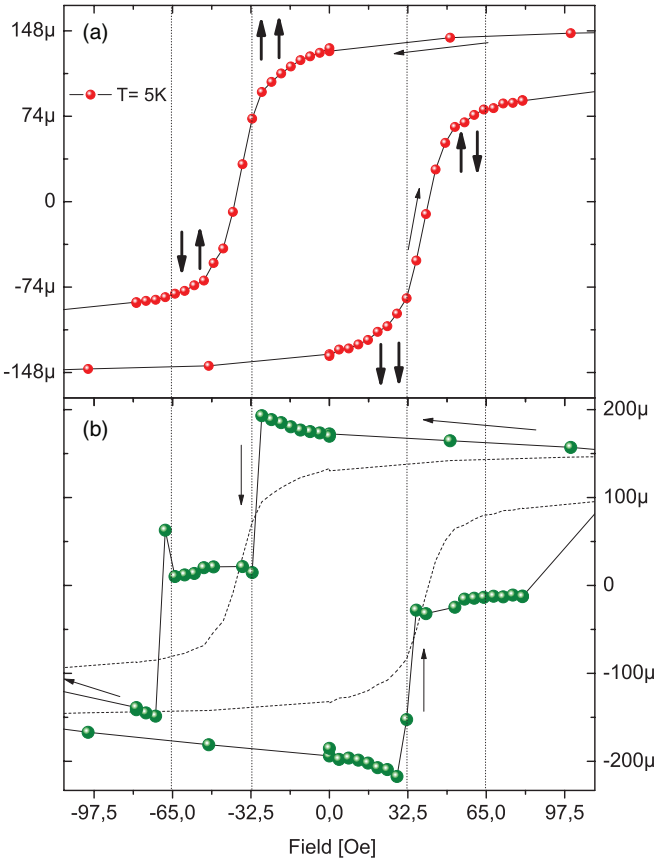

FIG. 3. (Color online) Zoom view of Ni(3)/Nb(25)/Ni(3)/CoO hysteresis loop shown in Fig. 2. (a) Magnetic hysteresis loop above T_c—bold arrows indicate relative magnetic orientation of the F layers. (b) Hysteresis loop of the superconducting magnetization.

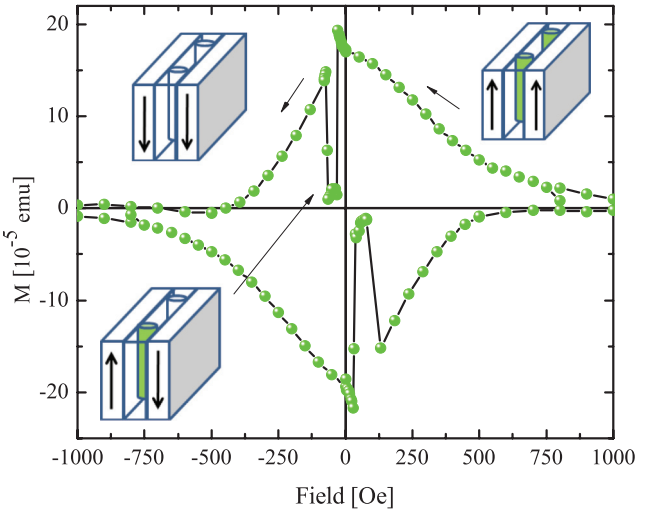

FIG. 4. (Color online) Modified magnetization (M) curve obtained by taking the absolute value of hysteresis loop in Fig. 2(b) for magnetization on increasing field (positive or negative fields) after vortex flipping occurs. Insets illustrate vortex dynamics in three different field ranges; dark (green) and clear (white) colors correspond to opposite vortex orientation.

pinned Ni layer domain structure is gradually rotating toward the parallel configuration.

Note that although the hysteresis loop above T_c [Fig. 3(a)] indicates a gradual rotation of the pinned layer, vortex flipping occurs in an abrupt way. This shows that a fully parallel configuration of the F layers is not needed in order to flip the remaining vortices. This could be explained as vortices may well see the average effect of the magnetization of each of the ferromagnetic layers. Thus, when the net magnetization of the pinned layer is on average negative, vortices flip to the negative direction. This occurs even though the pinned ferromagnet still has some domains pointing in the positive direction.

Finally, when the magnitude of the negative field is further increased, the number of vortices in the field direction increases due to vortex creation phase until the sample is filled with flux in the negative field direction. This leads to nearly zero net magnetization.

Stray field effects can be neglected: at high fields, vortices are in the applied field direction along ferromagnet magnetization. In this configuration, dipole fields, acting on the superconducting layer, point in the opposite direction of magnetization. When one of the Ni layers switches direction, the dipole field distribution changes, giving a net magnetic field intensity much smaller or nearly zero between the ferromagnets. The key point here is that vortex direction, determined from our data, is always along the magnetization direction, which is opposite to what one would expect from stray fields effects.

In order to verify our interpretation of the results and further analyze our data, we look only at the absolute value of magnetization, neglecting the "vortex flipping effect" (i.e., taking the absolute values of magnetization for measurements on the increasing field direction—positive or negative fields—after vortex flipping occurs).[31] Surprisingly, by this simple mathematical manipulation, one finds a curve, as shown in Fig. 4, similar to that in Fig. 1 and thus much simpler to interpret. Here it is easy to see that the magnetization curve looks almost like a conventional magnetization curve for a type II superconductor, with one important exception. Because vortex flipping takes place, the conventional vortex annihilation process is absent, leaving the system with three dominant vortex processes: vortex pinning, vortex flipping, and vortex creation, as shown in Fig. 4. Insets in this figure represent each of these processes; the vortex orientation, along the positive or negative field direction, is sketched by green or white, respectively (online version).

One may differentiate between vortex pinning and vortex creation phases by looking at the slope of the magnetization curves of Figs. 2(b) and 4 (slope vortex pinning $\sim 0.02 <$ slope vortex creation ~ 0.04).

On reducing the field, starting from high positive fields, Fig. 4 shows a nearly linear increase in magnetization. When switching the field to negative values, vortex flipping immediately occurs, followed by a vortex creation phase, starting initially very fast and moving more slowly until reaching saturation fields, as indicated from the diminishing slope of the curve.

With increasing field, from a large negative value toward zero, the vortex pinning process starts again, associated with the nearly linear increase in magnetization.

Finally, it is important to compare Figs. 1 and 4. One may differentiate between a vortex creation-annihilation process (Fig. 1) and a vortex creation process (Fig. 4) by looking at the slope of the magnetization curve branches with increasing field magnitude. Clearly the vortex creation process shows a greater slope (∼0.04) compared with the conventional vortex creation-annihilation process (∼0.01).

C. Co/Nb/Co/CoO spin valve structures

Our Nb/Co sputtered bilayer structure did not show the vortex flipping effect. In order to further investigate this, a Co/Nb/Co/CoO multilayered structure was measured.

As we shall explain, the magnetization measurements of this multilayered structure showed anisotropic pinning. This means that the pinning field depends on field direction.

For simplicity, we will refer to this structure as F1/S/F2/AF, where F1 is the free layer, and F2 corresponds to the pinned layer via exchange by the AF layer.

Cooling the sample at zero field while recording magnetization as a function of temperature gave a T_c value of 4.85 K.

Magnetization data of this sample measured above and below T_c at temperatures of 10 K and 2 K, respectively, is shown in Fig. 5. Above T_c, the hysteresis loop (continuous line) indicates that the F2 layer is strongly pinned along the positive field direction; therefore, a field in the negative field direction of about −3900 Oe is needed in order to un-pin the F2 layer. On the other hand, along the negative field direction, F2 is only weakly pinned, requiring a positive field of about 1800 Oe to switch its direction. This anisotropy in pinning field direction is an important difference compared with the Ni(3)/Nb(25)/Ni(3)/CoO(2)/Nb(4) sample, in which the Ni layer is equally pinned at both positive and negative fields.

Cooling the sample below T_c allows us to investigate the effects on the pinning field due to the superconducting phase. In the superconducting regime, Fig. 5 is analyzed along four field regions, A, B, C, and D, each representing a different ferromagnet magnetization orientation: A and C being parallel and B and D being antiparallel, as indicated with bold arrows in Fig. 5.

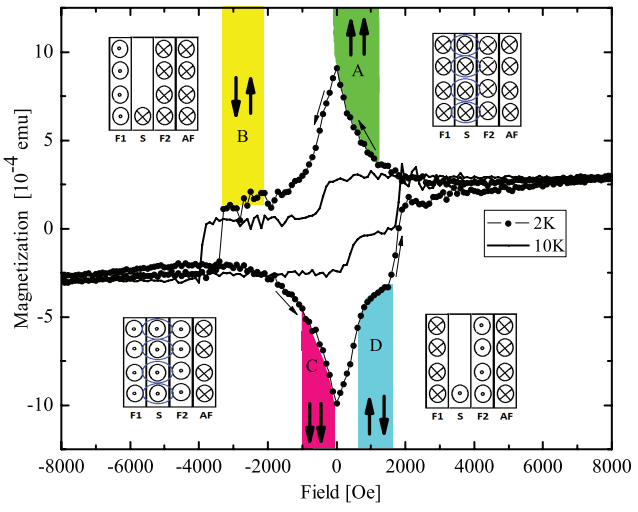

FIG. 5. (Color online) Magnetic hysteresis loop measured along the plane of Co(2.5)/Cu(5)/Nb(25)/Cu(5)/Co(2.5)/CoO(2.5)/Al(10) with anisotropic pinning. The measurements were taken above (continuous line) and below T_c (dark circles). Inset shows a schematic representation of the vortex and domain orientation within four field regions: A, B, C, and D.

The magnetization measurements taken at 2 K when Nb is in the superconducting state indicate a clear reduction of the F2 layer pinning field of about 400 Oe at negative fields. The pinning field of the F2 layer in the positive field direction does not appear to be affected much by the superconducting state. Again, this data does not show the vortex flipping effect, as in the case of Nb/Co bilayers.

In order to interpret these results, a schematic representation of the vortex and domain orientation within each of the four field regions is shown as insets in Fig. 5. These illustrations display the sample cross section corresponding to the plane perpendicular to the applied field direction. The symbols "⊗" and "⊙" represent opposite vortex or magnetic domain orientation in the superconductor or ferromagnets, respectively. Here "⊗" corresponds to the positive field direction and "⊙" to the negative field direction. The blue ovals portray vortex current penetration in neighboring ferromagnets. For the AF layer, the depicted orientation indicates the dominant pinning direction.

At field region B, the F2 layer magnetization is oriented along the dominant AF pinning direction, and flux trapping in the S layer is small, as given by the low magnetization values. Also, the F2 layer has an opposite magnetic orientation with respect to the F1 layer. Due to weak flux trapping at this field region, electron spins near the F2 interface only weakly experience magnetic field vortices. In this state, we observe a reduction in the ferromagnet pinning field of about 400 Oe. At larger negative fields, the F2 layer switches direction to an opposite one to the dominant AF pinning direction.

When we look at the positive field direction on the return branch of the hysteresis loop above field region D, only a much smaller decrease in coercive field of F2 is observed. Applying a positive field leaves the multilayered system with the same magnetic orientations for all layers (region A).

IV. INTERPRETATION OF THE RESULTS

A. Vortex flipping effect

Our experiments show experimental evidence of vortex flipping in F/S/F/AF spin valve structures. These results cannot be explained in terms of dipole stray fields, given the fact that these point in opposite direction to magnetization, while our data indicate that vortices always point in the magnetization direction (see Fig. 2).

In order to understand these results, we need to inquire about our system dimensions. As we mentioned earlier, we can estimate the order of the Ginzburg Landau coherence length $\xi_{GL} \sim 19$ nm. This corresponds to the vortex core radius. This estimate gives a vortex core diameter, $2\xi_{GL}$, ∼38 nm larger than the total Ni/Nb/Ni thickness of ∼31 nm. Certainly a vortex core in our sample can only extend into the ferromagnet up to the ferromagnetic coherence length. This gives an actual vortex core diameter of about $d_S + 2\xi_F$, where d_S is the superconductor thickness.

Considering that for Ni, the ferromagnetic coherence length is $\xi_{Ni} \sim 1.2$ nm, we expect vortex orbital currents to extend to almost half the entire ferromagnet's thickness. These currents circle around the ferromagnet's polarized electrons. In this scenario, electrons in the ferromagnet must experience the vortex magnetic field $B_v \sim 4\phi_o/\pi(d_S + 2\xi_F)^2$, where ϕ_o is the vortex flux quantum. If we assume that each electron has a magnetic moment of about 1 Bohr magneton μ_B, the torque exerted on each electron by the vortex field is $\mu_B \times B_v$. By Newton's third law, there is also a torque in the opposite direction exerted on vortex orbital currents. The energy associated with this torque is given by $-\mu_B \cdot B_v$, which will be minimized when the vortex magnetic moment points in the same direction as the electron spin.

Now let us analyze this situation in more detail. For simplicity, consider a S/F bilayer system. Leakage of vortex currents can only occur for the case where the vortex diameter $2\xi_{GL} > d_S$. This orbital current penetration is limited by proximity effect via ξ_F, leading to an actual vortex diameter equal to $d_S + \xi_F$. This assumes $\xi_F \leqslant d_F$, the ferromagnet thickness. Furthermore, we can express its magnetization in terms of sample dimensions and proximity parameters as

$$M = N\mu_B/(wl\xi_F), \tag{1}$$

where N is the electron polarization given by the difference of electron number in the ferromagnet with spin up and spin down, and w and l represent sample width and length, respectively.

Consider the case where the superconductor is completely filled up with N_o vortices. Let N electrons within the thickness range ξ_F be under the influence of the vortex magnetic field. By estimating the vortex field in terms of sample width w and vortex diameter $d_S + \xi_F$, we can assess the energy associated with this situation as

$$U = -(N\mu_B) \cdot [N_o\phi_o/w(d_S + \xi_F)], \tag{2}$$

where the first term in parenthesis is the magnetic moment and the second term the flux density. Using Eq. (1), we can express this energy in terms of magnetization by inserting ξ_F and l into Eq. (2). Furthermore, considering every vortex has a quantized magnetic moment, $\mu_v \sim \phi_o\, l/8\pi$,[32] Eq. (2) can also be written as

$$U = -8\pi N_o\mu_v M\xi_F/(d_S + \xi_F), \tag{3}$$

where the ratio $M\xi_F/(d_S + \xi_F)$ is a material parameter.

Equation (3) shows that the energy is minimized when the ferromagnet polarized electrons and vortex magnetic moments point along the same direction. This mechanism explains the vortex flipping effect.

The fact that electron magnetic moments in a ferromagnet all point in the same direction, due to the exchange field, result in a large torque exerted on orbital currents. This torque is also proportional to the number of trapped vortices. Note that if electrons where not coupled via exchange interaction, the net torque would be zero due to random spin orientation. Since electron spins are aligned by the exchange field, the net torque is N times larger.

The reason why this effect was not previously observed in Ref. 17 is because the superconductor thickness was greater than the vortex diameter $2\xi_{GL} < d_S$, where electrons in the ferromagnet are away from vortex magnetic field influence. This result was confirmed in our Nb/Co bilayer, where $2\xi_{GL} < d_S$ as a result of the shorter mean free path of the Nb sputtered layer that leads to a smaller ξ_{GL}.

Finally, our experiment on an e-beam Nb/Co multilayer, where $2\xi_{GL} > d_S$, as a result of a longer mean free path of the Nb layer, did not show the vortex flipping effect. Instead, a reduction of pinning field was observed when Nb was in the superconducting state.

In all experiments, vortex flipping was only observed whenever Ni was used as a ferromagnet. Equation (3) indicates that even for the case of a relatively thin Nb film, the increase in energy under vortex fields depends strongly on the type of ferromagnet used. A detailed theoretical investigation is needed in order to clearly quantify the minimum value of energy required for vortex flipping. This is beyond the scope of this investigation; however, using Eq. (3), it is possible to estimate the energy ratio U_{F1}/U_{F2} of two samples with the same superconductor thickness but different types of ferromagnet, F_1 or F_2:

$$U_{F1}/U_{F2} = M_{F1}\,\xi_{F1}\,(d_S + \xi_{F2})\,/M_{F2}\,\xi_{F2}\,(d_S + \xi_{F1}). \tag{4}$$

Taking, for example, parameters M and ξ_F for the materials Co and Ni, we find an energy ratio $U_{Co}/U_{Ni} \sim 0.4$, indicating that the associated energy for Co is much smaller than that for Ni.

This result shows that the vortex flipping effect is a direct consequence of two parameters; ξ_F, the measure of the proximity effect, and M, related to the exchange field. When using Co, the short Cooper pair penetration indicates a weak vortex penetration, leading to fewer electrons in the ferromagnet being under the influence of the vortex field.

B. Pinning field reduction effect

The experiment on the F1/S/F2/AF sample with anisotropic pinning shows an effective reduction of the F2 pinning field of about 400 Oe below T_c. As we will argue, this effect cannot be explained as the result of a vortex field acting on electrons in the ferromagnet. Consider the negative field region B around which the reduction of the pinning field occurs. Since the sample magnetic moment is slightly greater than zero, only a few vortices with $\phi_o > 0$ are trapped (i.e., point in the direction opposite the applied field). This reduces the effective field on F2, and therefore an increase of the pinning field is expected. The experimental result is clearly opposite, leaving out any explanation in terms of vortex field effects.

V. SUMMARY AND CONCLUSIONS

A detailed study of the magnetic properties of spin valve structures (F/S/F/AF) have been investigated in which one of the F layers is pinned. In these structures, the S layer thickness was chosen such that it is smaller than the vortex core diameter. Under this condition, vortex currents penetrate the neighboring ferromagnets. This work considers two distinct types of ferromagnets: Ni or Co.

For the case of Ni, the observed hysteresis loop is explained as a result of direct interaction of the superconducting

vortex magnetic field with the ferromagnet electrons. This interaction is strong enough that is able to "flip" vortices in the superconductor. These vortices appear to be equally influenced by each of the ferromagnets on the sides.

The results we report here constitute experimental evidence of a mechanism of interaction between vortices and ferromagnet electrons in S/F heterostructures as a direct consequence of the proximity effect. In this spin valve structure, three separate vortex processes are observed: vortex pinning, vortex flipping, and vortex creation. One may differentiate between vortex pinning and vortex creation phases by the slope of the magnetization curves, where in the former case the slope is clearly smaller than the later one. Also, as a result of the vortex flipping mechanism, these devices only exhibit a vortex creation phase, compared with a conventional superconductor with a vortex creation-annihilation process.

The experiment here, in which a vortex flipping process replaces a vortex annihilation process, differs from conventional superconductors, in which an external magnetic field applied in the direction opposite vortex orientation, no matter how strong it may be, is not able to "flip" a vortex. This is because such a field first creates a vortex that subsequently annihilates previous vortices of opposite sense trapped inside the material. In our device, however, vortex flipping is possible due to vortex fields acting on ferromagnetically aligned electrons through exchange interaction. This characteristic may find applications in reducing AC losses[33,34] and preventing flux jumps.[28]

Provided superconductor thickness is on the order of the Ginzburg Landau coherence length and the ferromagnet's exchange field is low, in order to have a large Cooper pair penetration, this effect should be observable in other materials. Such a mechanism has been made possible by fabrication of the F/S/F/AF multilayered spin valves with an S layer thin enough to barely confine vortices inside, as well as F layers thin enough to align and control magnetization within the plane.

When Co is used as a ferromagnet, there is no observed vortex flipping effect. This is attributed to the fact that Co has as shorter coherence length. Interestingly, a reduction in pinning field of about 400 Oe is observed when the Nb layer is in the superconducting state. This effect cannot be explained in terms of vortex fields. In view of these facts, any explanation must be directly related to the proximity effect and thus a phenomenon that deserves further investigation.

ACKNOWLEDGMENTS

We acknowledge technical support from G. Eguchi. This work was partially supported by a Grant-in-Aid for the Global COE program "The Next Generation of Physics, Spun from Universality and Emergence" and for the Scientific Research on Innovative Areas "Topological Quantum Phenomena" (No. 22103002) from MEXT of Japan. E.J.P. acknowledges "Programa Nacional de Ciencias Básicas" COLCIENCIAS (No. 120452128168).

[1] J. Xia, V. Shelukhin, M. Karpovski, A. Kapitulnik, and A. Palevski, Phys. Rev. Lett. **102**, 087004 (2009).
[2] R. I. Salikhov, N. N. Garif'yanov, I. A. Garifullin, L. R. Tagirov, K. Westerholt, and H. Zabel, Phys. Rev. B **80**, 214523 (2009).
[3] R. I. Salikhov, I. A. Garifullin, N. N. Garif'yanov, L. R. Tagirov, K. Theis-Bröhl, K. Westerholt, and H. Zabel, Phys. Rev. Lett. **102**, 087003 (2009).
[4] M. Lange, M. J.Van Bael, Y. Bruynseraede, and V. V. Moshchalkov, Phys. Rev. Lett. **90**, 197006 (2003).
[5] P. Fulde and R. A. Ferrell, Phys. Rev. **135**, A550 (1964).
[6] A. Larkin and Y. Ovchinnikov, Sov. Phys. JETP **20**, 762 (1965).
[7] J. S. Jiang, D. Davidović, D. H. Reich, and C. L. Chien, Phys. Rev. Lett. **74**, 314 (1995).
[8] L. Lazar, K. Westerholt, H. Zabel, L. R. Tagirov, Y. V. Goryunov, N. N. Garif'yanov, and I. A. Garifullin, Phys. Rev. B **61**, 3711 (2000).
[9] I. A. Garifullin, D. A. Tikhonov, N. N. Garif'yanov, L. Lazar, Y. V. Goryunov, S. Y. Khlebnikov, L. R. Tagirov, K. Westerholt, and H. Zabel, Phys. Rev. B **66**, 020505 (2002).
[10] V. Zdravkov, A. Sidorenko, G. Obermeier, S. Gsell, M. Schreck, C. Müller, S. Horn, R. Tidecks, and L. R. Tagirov, Phys. Rev. Lett. **97**, 057004 (2006).
[11] J. Zhu, I. N. Krivorotov, K. Halterman, and O. T. Valls, Phys. Rev. Lett. **105**, 207002 (2010).
[12] V. V. Ryazanov, V. A. Oboznov, A. Y. Rusanov, A. V. Veretennikov, A. A. Golubov, and J. Aarts, Phys. Rev. Lett. **86**, 2427 (2001).
[13] T. Kontos, M. Aprili, J. Lesueur, and X. Grison, Phys. Rev. Lett. **86**, 304 (2001).
[14] T. S. Khaire, M. A. Khasawneh, W. P. Pratt, Jr., and N. O. Birge, Phys. Rev. Lett. **104**, 137002 (2010).
[15] J. W. A. Robinson, J. D. S. Witt, and M. G. Blamire, Science **329**, 59 (2010).
[16] P. V. Leksin, N. N. Garif'yanov, I. A. Garifullin, Y. V. Fominov, J. Schumann, Y. Krupskaya, V. Kataev, O. G. Schmidt, and B. Büchner, Phys. Rev. Lett. **109**, 057005 (2012).
[17] S. Kobayashi, H. Oike, M. Takeda, and F. Itoh, Phys. Rev. B **66**, 214520 (2002).
[18] S. Kobayashi, Y. Kanno, and F. Itoh, Physica B **329**, 1357 (2003).
[19] E. J. Patiño, C. Bell, and M. G. Blamire, Eur. Phys. J. B **68**, 73 (2009).
[20] C. T. Hsieh, J. Q. Liu, and J. T. Lue, Appl. Surf. Sci. **252**, 1899 (2005).
[21] M. Lohndorf, A. Wadas, H. A. M. van den Berg, and R. Wiesendanger, Appl. Phys. Lett. **68**, 3635 (1996).
[22] S. Methfessel, S. Middelhoek, and H. Thomas, IBM J. Res. Dev. **4**, 96 (1960).
[23] H. W. Weber, E. Seidl, C. Laa, E. Schachinger, M. Prohammer, A. Junod, and D. Eckert, Phys. Rev. B **44**, 7585 (1991).
[24] T. Kontos, Ph.D. thesis, Université Paris XI Orsay, 2002.
[25] J. W. A. Robinson, S. Piano, G. Burnell, C. Bell, and M. G. Blamire, Phys. Rev. Lett. **97**, 177003 (2006).
[26] Š. Pick, I. Turek, and H. Dreyssé, Solid State Commun. **124**, 21 (2002).

[27]Estimated from the expression $\xi_{Cu} = (\hbar D_{Cu}/2\pi k_b T)^{1/2}$ at temperature $T = 6$ K and a diffusion coefficient for Copper $D_{Cu} = 20 \times 10^{-3}$ m^2/s.

[28]J. E. Evetts, A. M. Campbell, and D. Dew-Hughes, Phylos. Mag. **10**, 339 (1964).

[29]This transition corresponds to the 25-nm Nb film. The capping Nb layer did not show superconductivity in experimental temperature range.

[30]J. B. Yi, J. Ding, B. H. Liu, Z. L. Dong, T. White, and Y. Liu, J. Magn. Magn. Mater. **285**, 224 (2005).

[31]$M = -\{M(1.8\text{ K}) - M(5\text{ K})\}$ for $|H| > |H_{\text{vortex-flip}}|$, for the magnetization curve branches with increasing magnitude of H; $M = M(1.8\text{ K}) - M(5\text{ K})$ otherwise. Here, $H_{\text{vortex-flip}}$ is the field at which vortex flipping occurs.

[32]L.-P. Levy, *Magnetism and Superconductivity* (Springer, Paris, 1997).

[33]J. R. Clem, J. Appl. Phys. **50**, 3518 (1979).

[34]G. Lukovsky, A. Friedman, Y. Wolfus, L. Burlachkov, and Y. Yeshurun, IEEE Trans. Appl. Supercond. **17**, 3137 (2007).